

Synthesis, IR, UV–vis spectra, x-ray diffraction and band structure of a non-centrosymmetric borate single-crystal $\text{CaBiGaB}_2\text{O}_7$

This article has been downloaded from IOPscience. Please scroll down to see the full text article.

2009 J. Phys.: Condens. Matter 21 205402

(<http://iopscience.iop.org/0953-8984/21/20/205402>)

View [the table of contents for this issue](#), or go to the [journal homepage](#) for more

Download details:

IP Address: 129.252.86.83

The article was downloaded on 29/05/2010 at 19:43

Please note that [terms and conditions apply](#).

Synthesis, IR, UV–vis spectra, x-ray diffraction and band structure of a non-centrosymmetric borate single-crystal $\text{CaBiGaB}_2\text{O}_7$

Ali Hussain Reshak^{1,2,7}, Xuean Chen³, Fangping Song³, I V Kityk^{4,5}
and S Auluck⁶

¹ Institute of Physical Biology, South Bohemia University, Nove Hradý 37333, Czech Republic

² Institute of System Biology and Ecology, Academy of Sciences, Nove Hradý 37333, Czech Republic

³ College of Materials Science and Engineering, Beijing University of Technology, Ping Le Yuan 100, Beijing 100124, People's Republic of China

⁴ Department of Chemistry, Silesian University of Technology, ulica Marcina Strzody 9, PL-44100 Gliwice, Poland

⁵ Electrical Engineering Department, Czestochowa Technological University, Al. Armii Krajowej 17/19, Czestochowa, Poland

⁶ Physics Department, Indian Institute of Technology Kanpur, Kanpur (UP) 208016, India

E-mail: maalidph@yahoo.co.uk

Received 15 January 2009, in final form 29 March 2009

Published 24 April 2009

Online at stacks.iop.org/JPhysCM/21/205402

Abstract

A non-centrosymmetric borate, $\text{CaBiGaB}_2\text{O}_7$, has been grown by a solid-state reaction method at a temperature below 700 °C. The single-crystal x-ray structural analysis has shown that it crystallizes in the tetragonal space group $P4_21m$ with $a = 0.7457(1)$ nm, $c = 0.4834(1)$ nm, $Z = 2$. It has a three-dimensional (3D) structure in which $[\text{B}_2\text{O}_7]^{8-}$ groups are bridged by $[\text{GaO}_4]^{5-}$ tetrahedra through shared O atoms to form $2\text{D} \frac{2}{\infty}[\text{GaB}_2\text{O}_7]^{5-}$ layers that are further linked by $\text{Bi}^{3+}/\text{Ca}^{2+}$ cations giving rise to the final 3D framework. The IR spectrum confirms the presence of $[\text{BO}_4]^{5-}$ groups and the UV–vis diffuse reflectance spectrum shows that the optical band gap is about 2.9 eV. This value is compared with our band structure calculations using the full potential linearized augmented plane wave approach within the framework of the Engel–Vosko GGA formalism.

(Some figures in this article are in colour only in the electronic version)

1. Introduction

Borates have attracted considerable attention because they have important practical applications as materials for nonlinear optical (NLO) effects, in particular optical second harmonic generation (SHG) and linear electro-optics effects (EOE). For example, β - BaB_2O_4 , LiB_3O_5 , CsB_3O_5 and $\text{YCa}_4(\text{BO}_3)_3\text{O}$ are all well-known NLO materials [1]. The binary Bi_2O_3 – B_2O_3 phase diagram was investigated by Levin and McDaniel [2]

and at least five compounds were structurally characterized including $\text{Bi}_{24}\text{B}_2\text{O}_{39}$ [3], $\text{Bi}_4\text{B}_2\text{O}_9$ [4], $\text{Bi}_3\text{B}_5\text{O}_{12}$ [5], BiB_3O_6 [6] and $\text{Bi}_2\text{B}_8\text{O}_{15}$ [7]. Among them, $\text{Bi}_4\text{B}_2\text{O}_9$ was reported to have a high birefringence [8], $\text{Bi}_3\text{B}_5\text{O}_{12}$ displays stimulated Raman scattering and luminescence properties [9, 10], and BiB_3O_6 is the most extensively studied because it has been established as a NLO material with outstanding physical properties. Measurements of the piezoelectric, pyroelectric, dielectric, elastic and thermoelastic properties have been reported [11]. Theoretical studies

⁷ Author to whom any correspondence should be addressed.

have shown that the presence of irregular Bi–O coordination polyhedra and their structural arrangement lead to the extraordinarily large SHG effect in BiB_3O_6 . It is reasonable to believe that other interesting materials may also be found in more complex borates incorporating bismuth together with other metal elements. Based on this idea, several ternary (quaternary) bismuth-containing borates that crystallize in the non-centrosymmetric space groups have been recently synthesized, including BaBiBO_4 , $\text{Bi}_2\text{ZnB}_2\text{O}_7$, $\text{CaBiGaB}_2\text{O}_7$, $\text{Bi}_2\text{CaB}_2\text{O}_7$ and $\text{Bi}_2\text{SrB}_2\text{O}_7$ [12–14]. Among these, $\text{CaBiGaB}_2\text{O}_7$ was prepared in powder form and its crystal structure was determined from powder diffraction data using the Rietveld method [13].

The present study is aimed at synthesizing and characterizing the non-centrosymmetric borate, $\text{CaBiGaB}_2\text{O}_7$ and presenting calculations of the band structure and density of states using the full potential linear augmented plane wave (FP-LAPW) method. In the course of our systematic investigation of novel borate NLO materials, we have successfully isolated single crystals of $\text{CaBiGaB}_2\text{O}_7$ and redetermined its crystal structure using the single-crystal XRD technique. This structural information is used for the theoretical calculations. The FP-LAPW method has been proven to be one of the most accurate methods [15, 16] for the computation of the electronic structure of solids within the density functional theory (DFT) approach. This method has been applied to the calculations of many borates [17]. In addition, we have also measured the IR and UV–vis diffuse reflectance spectrum of this compound. To the best of our knowledge there are no experimental measurements of XRD, IR and UV–vis and no first principles calculations on the non-centrosymmetric borate, $\text{CaBiGaB}_2\text{O}_7$. Therefore a combined experimental and theoretical study of the non-centrosymmetric borate, $\text{CaBiGaB}_2\text{O}_7$ is timely and would help in understanding the origin of its electronic properties. In section 2 we present details of the crystal growth, structural features and theoretical calculations. Section 3 presents the energy bands and a comparison with the experimental data with the appropriate discussion.

2. Experiment and theory

2.1. Crystal growth and general characterization

For the preparation of the compound in the title, a powder mixture of 1.3274 g CaCO_3 , 3.0898 g Bi_2O_3 , 1.2429 g Ga_2O_3 and 4.9200 g H_3BO_3 (the $\text{CaO}/\text{Bi}_2\text{O}_3/\text{Ga}_2\text{O}_3/\text{B}_2\text{O}_3$ molar ratio = 2:1:1:4) was transferred to a small gold crucible. The sample was gradually heated to 665 °C, where it was kept for two weeks, then cooled down to 550 °C at a rate of 5 °C h⁻¹, followed by cooling to room temperature at a rate of 20 °C h⁻¹. The colorless, tetragonal, plate-like crystals of $\text{CaBiGaB}_2\text{O}_7$ were found to grow on the surface of the sample. Several small crystals could be isolated mechanically from the reaction product for further characterization by single-crystal XRD measurements. Subsequently, direct reaction of a stoichiometric mixture of Bi_2O_3 , Ga_2O_3 , CaCO_3 and H_3BO_3 at 600 °C for two weeks with several intermediate remixings

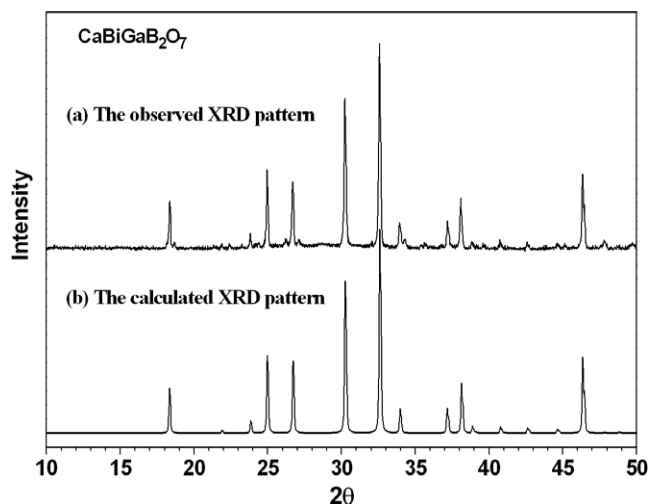


Figure 1. XRD pattern of $\text{CaBiGaB}_2\text{O}_7$ observed from a powder polycrystalline sample (a) and calculated from the single-crystal data (b).

yielded a single-phase polycrystalline sample of $\text{CaBiGaB}_2\text{O}_7$, as confirmed by powder x-ray analysis using monochromatic $\text{Cu K}\alpha$ radiation from a Bruker D8 ADVANCE diffractometer (figure 1).

Infrared spectra were recorded from 4000 to 400 cm^{-1} on a Perkin Elmer 1730 FT-IR spectrometer from KBr pellets. Optical diffuse reflectance spectra were measured at room temperature with a Shimadzu UV-3101PC double-beam, double-monochromator spectrophotometer. Data were collected in the wavelength range 200–800 nm. BaSO_4 powder was used as a standard (100% reflectance). A similar procedure, as previously described [18], was used to collect and convert the data using the Kubelka–Munk function [19].

2.2. Structural parameters

Single-crystal x-ray intensity data were collected at room temperature (298 K) on an automated Rigaku AFC7R four-circle diffractometer using monochromatic $\text{Mo K}\alpha$ radiation. The cell dimensions were obtained from a least-squares refinement with 25 automatically centered reflections in the range $41.06^\circ \leq 2\theta \leq 44.80^\circ$. Three standard reflections were remeasured after every 150 reflections and no decay was observed. The raw intensity data were corrected for Lorentz and polarization effects and for absorption by an empirical method based on ψ -scan data.

The crystal structure was solved by a direct method and refined in the SHELX-97 system [20] by full-matrix least-squares methods on F_o^2 . The refinement of 34 parameters with 495 observed reflections ($I \geq 2\sigma(I)$) resulted in the residuals of $R1/wR2 = 0.0398/0.1086$. The final difference electron density maps were featureless, with the highest electron density of $1.52 \text{ e } \text{\AA}^{-3}$ at a position that is very close to the heavy atomic site (Bi/Ca). Details of crystal parameters, data collection and structure refinements are given in table 1 and the atomic coordinates and the equivalent isotropic displacement parameters are summarized in table 2.

Table 1. Crystallographic data for CaBiGaB₂O₇.

Chemical formula	CaBiGaB ₂ O ₇
Space group	$P\bar{4}2_1m$ (No. 113)
a (nm)	0.7457(1)
c (nm)	0.4834(1)
V (nm ³), Z	0.268 80(8), 2
d_{calc} (g cm ⁻³)	5.589
$\lambda_{\text{Mo K}\alpha}$ (nm)	0.071 073
μ (mm ⁻¹)	38.638
$2\theta_{\text{max}}$	64.88°
Unique reflections	535
Observed ($I \geq 2\sigma(I)$)	495
No. of variables	34
GOF on F^2	1.100
$R1/wR2$ ($I \geq 2\sigma(I)$)	0.0398/0.1086
$R1/wR2$ (all data)	0.0428/0.1096

Table 2. Atomic coordinates ($\times 10^4$) and equivalent isotropic displacement parameters (nm² $\times 10^6$) for CaBiGaB₂O₇. (Note: U_{eq} is defined as one third of the trace of the orthogonalized U tensor.)

Atoms	X	Y	Z	U_{eq}
Bi/Ca	6716(1)	1716(1)	9998(2)	24(1)
Ga	5000	5000	5000	9(1)
B	3692(12)	1308(12)	5539(19)	15(2)
O1	5000	0	6490(20)	13(2)
O2	3559(7)	1441(7)	2561(12)	12(1)
O3	4233(8)	3080(8)	7006(12)	18(1)

2.3. Theoretical calculations

The single-crystal x-ray structural analysis showed that CaBiGaB₂O₇ crystallizes in the tetragonal space group $P\bar{4}2_1m$ with lattice constants $a = 0.7457(1)$ nm, $c = 0.4834(1)$ nm, $Z = 2$. We have performed calculations of the electronic properties applying the full potential linearized augmented plane wave (FP-LAPW) method as incorporated in the WIEN2K code [21]. This is an implementation of density functional theory (DFT) [22] with different possible approximations for the exchange correlation (XC) potentials. The exchange correlation potential was calculated using the Engel–Vosko GGA formalism [23], which optimizes the corresponding potential for band structure calculations. It is well known that in the self-consistent band structure calculation within the DFT approach, both LDA and GGA usually underestimate the energy gap [24]. This is mainly due to the fact that they have simple forms that are not sufficiently flexible to accurately reproduce both the exchange correlation energy and its charge derivative. Engel and Vosko considered this shortcoming and constructed a new functional form of GGA [23] which is better able to reproduce the exchange potential at the expense of less agreement in the exchange energy. This approach, called EV-GGA, yields more accurate band splittings.

In order to achieve energy eigenvalue convergence, the wavefunctions in the interstitial regions were expanded as plane waves with a cut-off $K_{\text{max}} = 9/R_{\text{MT}}$, where R_{MT} denotes the smallest atomic sphere radius and K_{max} gives the magnitude of the largest K vector in the plane wave expansion. The muffin-tin radii were assumed to be 2.14, 1.69 and 1.55

Table 3. Selected bond lengths (nm) and angles (°) for CaBiGaB₂O₇.

Bi/Ca–O2	0.2304(7)	Ga–O3 \times 4	0.1822(5)
Bi/Ca–O3 \times 2	0.2375(6)		
Bi/Ca–O1	0.2480(7)	B–O2	0.1447(10)
Bi/Ca–O3 \times 2	0.2560(6)	B–O1	0.1453(12)
Bi/Ca–O2 \times 2	0.2668(5)	B–O3 \times 2	0.1553(9)
O3–Ga–O3 \times 2	115.7(4)	O2–B–O1	114.0(9)
O3–Ga–O3 \times 4	106.47(18)	O2–B–O3 \times 2	114.4(6)
		O1–B–O3 \times 2	104.6(6)
		O3–B–O3	103.5(7)

atomic units (au) for Bi, Ga and Ca, respectively and 1.34 au for B and O. The valence wavefunctions inside the spheres are expanded up to $l_{\text{max}} = 10$ while the charge density was Fourier expanded up to $G_{\text{max}} = 14(\text{au})^{-1}$.

Self-consistency is obtained using 350 k -points in the irreducible Brillouin zone (IBZ). The electronic properties are calculated using 500 k -points in the IBZ. The self-consistent calculations were assumed to have converged when the total energy of the system stabilized within 10^{-5} Ryd.

3. Results and discussion

3.1. X-ray diffraction, IR and UV–vis diffuse reflectance spectrum

The crystal structure of CaBiGaB₂O₇ consists of two-dimensional (2D) gallium borate layers connected through O–Bi³⁺/Ca²⁺–O linkages to form a continuous three-dimensional (3D) framework, as depicted in figure 2. In this structure, two [BO₄]⁵⁻ tetrahedra are connected *via* the common O atom to form a [B₂O₇]⁸⁻ dimer. These [B₂O₇]⁸⁻ dimers are bridged by tetrahedral Ga³⁺ centers to generate a 2D infinite ${}^2_{\infty}[\text{GaB}_2\text{O}_7]^{5-}$ layer parallel to the (001) plane. The ${}^2_{\infty}[\text{GaB}_2\text{O}_7]^{5-}$ layers are stacked along the crystallographic c -axis and the Bi³⁺/Ca²⁺ cations are located between the layers to balance the charge and also to hold the layers together through Bi³⁺/Ca²⁺–O bonds.

Selected bond lengths and angles in CaBiGaB₂O₇ are listed in table 3 and the local Bi/Ca coordination geometry shown in figure 3. It is clear that bismuth and calcium atoms are statistically distributed over the crystallographic 4e sites and each is coordinated with eight oxygen atoms forming a distorted square anti-prismatic geometry. The Bi/Ca–O distances vary between 0.2304(7) and 0.2668(5) nm with a mean value of 0.2499 nm, which agrees well with the values 0.2500 and 0.2550 nm computed from crystal radii for a 8-coordinated Ca²⁺ and Bi³⁺ ion, respectively [25]. The Bi³⁺/Ca²⁺ disorder is unusual due to their very different coordination geometries, but it has been previously observed, e.g., in Ca₃Bi(PO₄)₃ [26], Ca₉Bi₃V₁₁O₄₁ [27], and Ca₄BiV₃O₁₃ [28]. All our attempts to refine the structure into lower-symmetry space groups with an ordered distribution of Bi and Ca atoms have failed. An examination of the CaBiGaB₂O₇ crystal with a slower scan rate and lower intensity limitation did not indicate any symmetry lower than tetragonal or a larger unit cell that would allow Bi/Ca ordering.

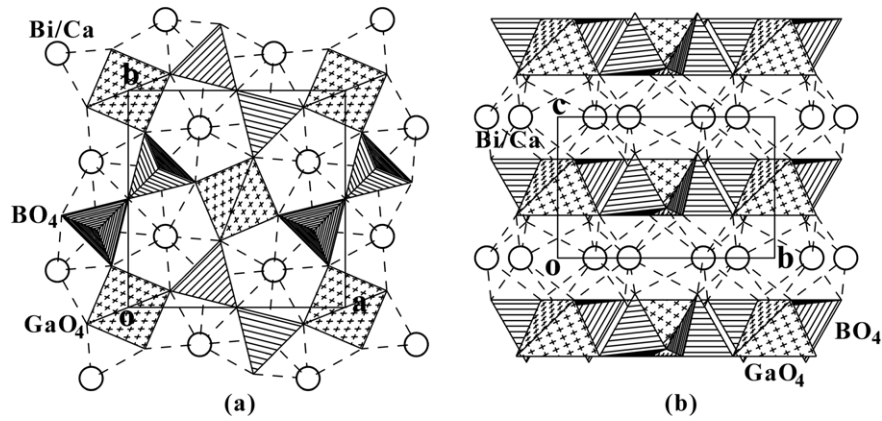


Figure 2. The crystal structure of $\text{CaBiGaB}_2\text{O}_7$ projected along the [001] (a) and [100] (b) direction, respectively, where tetrahedra with crosses are GaO_4 groups, tetrahedra with parallel lines are BO_4 groups and the open circles are Bi/Ca atoms.

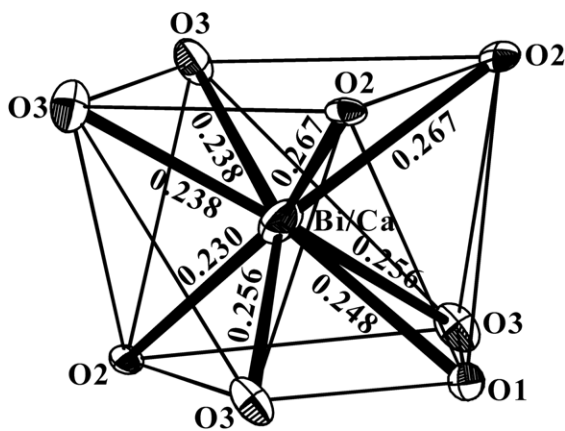


Figure 3. Coordination geometry about the Bi/Ca atom, where Bi/Ca–O distances are shown in units of nm and the displacement ellipsoids drawn at the 50% probability level.

Therefore, the $\text{Bi}^{3+}/\text{Ca}^{2+}$ disorder model was finally assumed. This model has also been confirmed by the powder diffraction results (figure 1 and [13]).

There is one crystallographically independent Ga and one distinct B atom in the asymmetric unit, both having a typical tetrahedral oxygen ligand environment (see figure 2 and table 3). The Ga atom is located on a crystallographic $\bar{4}$ axis, giving a single Ga–O bond distance ($4 \times 0.1822(5)$ nm) and two sets of O–Ga–O angles ($2 \times 115.7(4)^\circ$ and $4 \times 106.47(18)^\circ$), while the B atom lies on a mirror plane, resulting in three sets of B–O bond lengths ($1 \times 0.1447(10)$ nm, $1 \times 0.1453(12)$ nm and $2 \times 0.1553(9)$ nm) and four sets of O–B–O angles ($1 \times 114.0(9)^\circ$, $2 \times 114.4(6)^\circ$, $2 \times 104.6(6)^\circ$ and $1 \times 103.5(7)^\circ$). These geometric parameters are comparable to those observed in the structures of $\text{K}_2\text{Ga}_2\text{O}(\text{BO}_3)_2$ [29] and $\text{Na}_3\text{ZnB}_5\text{O}_{10}$ [30], where GaO_4 and BO_4 groups were observed, respectively. Of the three unique O atoms, O1 and O2 lie on the crystallographically special positions with site symmetries $2m$ and m , respectively, while O3 occupies a general position. All of O atoms are four-coordinated, being bonded to 2B and 2Bi/Ca (for O1), 1B and 3Bi/Ca (for O2), or 1B, 1Ga and 2Bi/Ca (for O3) centers to constitute distorted O-centered tetrahedra (tetrahedral angles are in the range

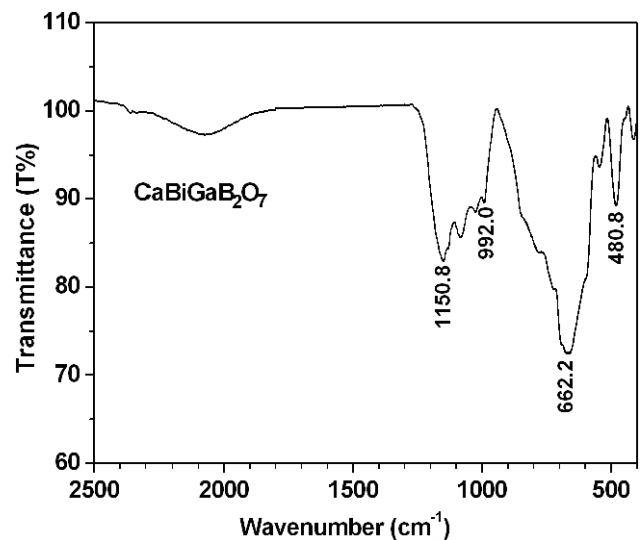


Figure 4. Infrared spectrum of $\text{CaBiGaB}_2\text{O}_7$.

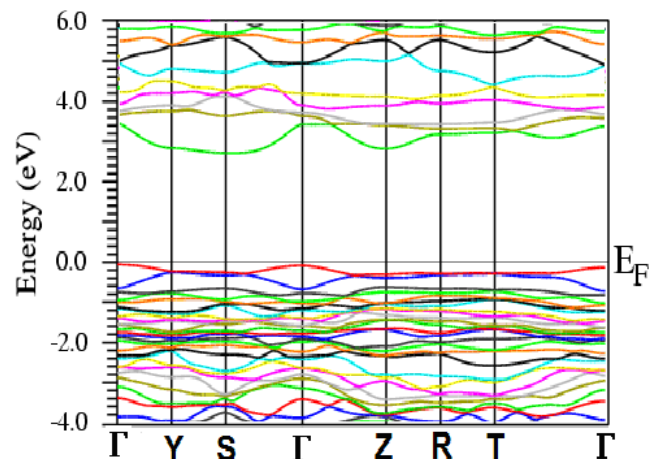


Figure 5. Calculated band structure of $\text{CaBiGaB}_2\text{O}_7$.

$85.4(2)^\circ$ – $143.2(9)^\circ$). Bond-valence sum calculations [31] produced values of 3.12 for Ga and 2.84 for B, consistent with their expected formal valences.

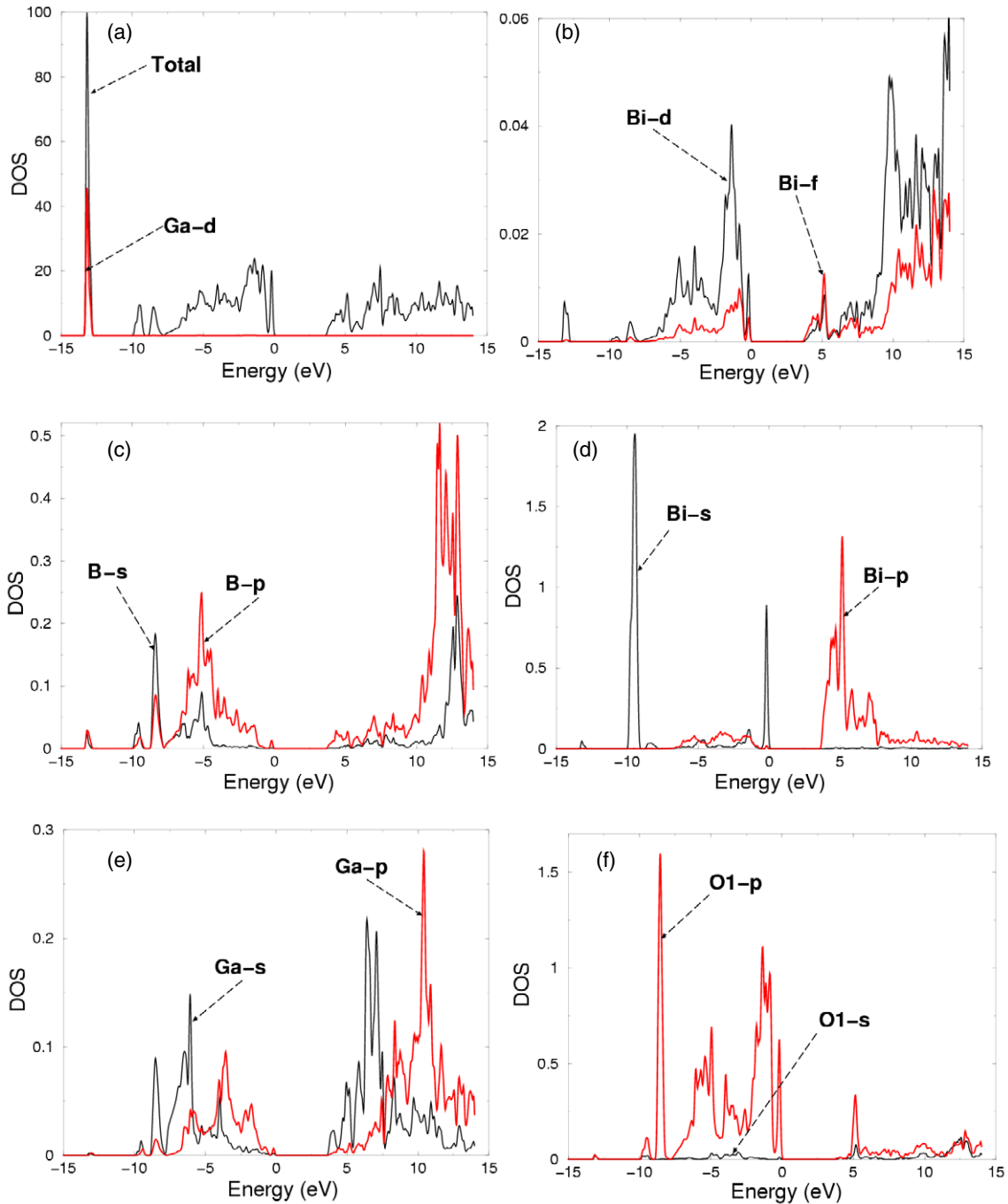


Figure 6. Total and partial density of states (states/eV unit cell) of $\text{CaBiGaB}_2\text{O}_7$ (a) Calculated total density of states along with Ga d partial density of states (states/eV unit cell). (b) Calculated Bi d and Bi f partial densities of states (states/eV unit cell). (c) Calculated B s and B p partial densities of states (states/eV unit cell). (d) Calculated Bi s and Bi p partial densities of states (states/eV unit cell). (e) Calculated Ga s and Ga p partial densities of states (states/eV unit cell). (f) Calculated O1 s and O1 p partial densities of states (states/eV unit cell) (as an exemplar we show only O1, the same is true for the others).

The crystal structure of $\text{CaBiGaB}_2\text{O}_7$ is closely related to, but different from that of $\text{Bi}_2\text{ZnB}_2\text{O}_7$ [13]. The latter consists of $[\text{B}_2\text{O}_5]^{4-}$ and $[\text{B}_2\text{O}_7]^{8-}$ groups that are formed by two corner-sharing BO_3 triangles and two corner-sharing BO_4 tetrahedra, respectively. The $[\text{B}_2\text{O}_5]^{4-}$ and $[\text{B}_2\text{O}_7]^{8-}$ groups are bridged by $[\text{ZnO}_4]^{6-}$ tetrahedra through shared O atoms to form $2\text{D } \infty[\text{ZnB}_2\text{O}_7]^{6-}$ layers that are further bridged by octahedrally coordinated Bi^{3+} cations, giving rise to the final

3D framework. In contrast, only $[\text{B}_2\text{O}_7]^{8-}$ groups as well as eight-fold coordinated $\text{Bi}^{3+}/\text{Ca}^{2+}$ cations are observed in $\text{CaBiGaB}_2\text{O}_7$. In fact, the crystal structure of $\text{Bi}_2\text{ZnB}_2\text{O}_7$ is derived from that of $\text{CaBiGaB}_2\text{O}_7$ in the following manner: $\text{CaBiGaB}_2\text{O}_7$ structure ($P4_21m$, a , c , $Z = 2$) \rightarrow hypothetical derivative ($Cmm2$, which is type I subgroup of $P4_21m$, $a - b$, $a + b$, c , $Z = 4$) \rightarrow $\text{Bi}_2\text{ZnB}_2\text{O}_7$ structure ($Pba2$, which is type IIa subgroup of $Cmm2$, $a - b$, $a + b$, c , $Z = 4$).

Concerning the IR spectra it is known [32] that four normal vibrations with frequencies ν_s (symmetric stretching) at 740–890 cm^{-1} , γ (symmetric bending) at 400–600 cm^{-1} , ν_{as} (asymmetrical stretching) at 1000–1150 cm^{-1} and δ (asymmetric bending) at about 600 cm^{-1} correspond to the $[\text{BO}_4]^{5-}$ tetrahedron. The infrared spectrum of $\text{CaBiGaB}_2\text{O}_7$ is presented in figure 4. It is clear that the bands with the frequencies of about 480.8 cm^{-1} may be assigned as the BO_4 symmetric bending vibrations (γ); the bands in the range 992.0–1150.8 cm^{-1} may be associated with the BO_4 asymmetric stretch (ν_{as}); and those around 662.2 cm^{-1} as due to the BO_4 asymmetric bending modes (δ). The BO_4 group in $\text{CaBiGaB}_2\text{O}_7$ is distorted from the ideal T_d symmetry. This removes the degeneracy of the infrared active vibrations (ν_{as} and δ) resulting in band splitting and also allows the non-active vibration γ to absorb energy in the infrared region. The IR spectrum confirms the existence of tetrahedrally coordinated boron atoms, consistent with the results obtained from the crystallographic study.

The optical diffuse reflectance spectrum measurements on the $\text{CaBiGaB}_2\text{O}_7$ polycrystalline sample revealed that the compound has a steep absorption edge, confirming the semiconducting nature, as expected from the electron count in the chemical formula. The optical band gap obtained by extrapolation of the linear part of the spectral absorption edge is equal to about 2.9 eV, consistent with the very pale yellow color of the sample.

3.2. Band structure and density of states

The band structure, total density of states (TDOS) along with the Bi *s/p/d/f*, B *s/p*, Ga *s/p/d* and O *s/p* partial (PDOS) for $\text{CaBiGaB}_2\text{O}_7$ are shown in figures 5 and 6. The valence band maximum (VBM) is located at Γ and the conduction band minimum (CBM) is located at halfway between S and the Γ point, resulting in an indirect energy gap of 2.9 eV. It should be emphasized that the energy gap is substantially lower than that for the other borates (3.4–5.1 eV) [33]. This fact may indicate the crucial role of the cationic sub-systems on the band edges of the borates.

The band structure and hence the density of states (DOS) can be divided into five principal groups/structures. From the PDOS we have identified the angular momentum character for the various structures. The lowest group (around –14.0 eV) originates from Ga *d* with small admixtures of B *s* and Bi *s* states. The second group around –10.0 eV has significant contributions from Bi *s* and very small admixtures of O *s/p*, Ga *s/p* and B *s/p* states. The third group (around –8.0 eV) is mainly of O *p* with a small contribution from B *s/p*, Bi *s* and Ga *s/p* states. The group from –7.0 eV up to the Fermi energy (E_F) is mainly of O *p* and Bi *s* with small contributions of O *s*, Ga *s/p*, Bi *p/d/f* and B *s/p* states. The groups from the CBM up to 15.0 eV are due to Bi *p* and O *s/p* with small contributions from Ga *s/p*, B *s/p* and Bi *d/f* states. The electronic structure of the upper valence band is dominated by the O *p* and B *s* states. We note that most of the O *p* character is concentrated in the upper valence band, with only negligible amounts in the conduction band. The CBM is controlled by Bi *p* states.

From the PDOS, we note that the Ga *s* states strongly hybridized with the B *s* states at around –5.0 eV, and Ga *p* with B *p* at around 10.0 eV. The Fermi energy is determined by the strong hybridization between Bi *s* and O *p* states. The main reason of the lower band energy edge, compared with other borates, is the existence of the Bi *p* and Ga *s* conduction sub-bands which are substantially narrow. Also the higher band energy shows more dispersion compared to other borates with the different cationic sub-systems. The observed changes are a consequence of the different cationic polarities and the different borate configurations; these changes could be used to control the band structure parameters in the desired directions.

4. Conclusions

A non-centrosymmetric borate with the composition $\text{CaBiGaB}_2\text{O}_7$ has been synthesized and the crystal structure, IR and UV–vis diffuse reflectance spectrum have been studied. This compound crystallizes in the tetragonal space group $P4_21m$ and has a 3D network consisting of ${}^2_{\infty}[\text{GaB}_2\text{O}_7]^{5-}$ layers bridged by eight-coordinated $\text{Bi}^{3+}/\text{Ca}^{2+}$ cations. For band structure calculations we have applied the EV-GGA exchange correlation potential within the DFT based FP-LAPW approach. Our calculations show that this compound has an indirect energy gap of 2.9 eV in agreement with our measured energy gap of 2.9 eV. This energy gap is smaller than the energy gap of other borates. This could be due to the existence of narrow Bi *p* and Ga *s* conduction sub-bands and a larger dispersion (lower effective masses) in the higher energy bands compared to other borates. We also note that the overlapping of the bands around the Fermi energy is determined by the strong hybridization between Bi *s* and O *p* states. In the energy range around –5.0 eV the Ga *s* states hybridize strongly with B *s* states and around 10.0 eV the Ga *p* states hybridize with B *p* states.

Acknowledgments

Ali Hussain Reshak acknowledges support in this work from the Institutional Research Concept of the Institute of Physical Biology, UFB (No. MSM6007665808) and the Institute of System Biology and Ecology, ASCR (No. AVOZ60870520). Xuean Chen acknowledges support from the Funding Project for Academic Human Resources Development in Institutions of Higher Learning under the jurisdiction of the Beijing Municipality and the National Natural Science Foundation of China (grant No. 20871012).

References

- [1] Becker P 1998 *Adv. Mater.* **10** 979
- [2] Levin E M and McDaniel C L 1962 *J. Am. Ceram. Soc.* **45** 355
- [3] Kargin Y F and Egorysheva A V 1998 *Inorg. Mater.* **34** 714
- [4] Hyman A and Perloff A 1972 *Acta Crystallogr. B* **28** 2007
- [5] Filatov S, Shepelev Y, Bubnova R, Sennova N, Egorysheva A V and Kargin Y F 2004 *J. Solid State Chem.* **177** 515
- [6] Frohlich R, Bohaty L and Liebertz J 1984 *Acta Crystallogr. C* **40** 343

- [7] Teng B, Yu W T, Wang J Y, Cheng X F, Dong S M and Liu Y G 2002 *Acta Crystallogr. C* **58** i25
- [8] Muehlberg M, Burianek M, Edongue H and Poetsch C 2002 *J. Cryst. Growth* **237–239** 740
- [9] Egorysheva A V, Burkov V I, Gorelick V S, Kargin Yu F, Koltashev V V and Plotnichenko B G 2001 *Fiz. Tverd. Tela* **43** 1590
Egorysheva A V, Burkov V I, Gorelick V S, Kargin Yu F, Koltashev V V and Plotnichenko B G 2001 *Phys. Solid State* **43** 1655 (Engl. Transl.)
- [10] Blasse G, Oomen E W J L and Liebertz J 1986 *Phys. Status Solidi b* **137** K77
- [11] Haussühl S, Bohatý L and Becker P 2006 *Appl. Phys. A* **82** 495
- [12] Barbier J, Penin N, Denoyer A and Cranswick L M D 2005 *Solid State Sci.* **7** 1055
- [13] Barbier J, Penin N and Cranswick L M 2005 *Chem. Mater.* **17** 3130
- [14] Barbier J and Cranswick L M D 2006 *J. Solid State Chem.* **179** 3958
- [15] Gao S 2003 *Comput. Phys. Commun.* **153** 190
- [16] Schwarz K 2003 *J. Solid State Chem.* **176** 319
- [17] Reshak A H, Auluck S and Kityk I V 2008 *J. Alloys Compounds* **460** 99–102
Reshak A H, Auluck S and Kityk I V 2007 *Phys. Rev. B* **75** 245120
- [18] Li J, Chen Z, Wang X-X and Proserpio D M 1997 *J. Alloys Compounds* **262/263** 28
- [19] Wendlandt W W M and Hecht H G 1966 *Reflectance Spectroscopy* (New York: Wiley-Interscience)
- [20] Sheldrick G M 1997 *SHELX-97: Program For Structure Refinement* University of Goettingen, Germany
- [21] Blaha P, Schwarz K, Madsen G K H, Kvasnicka D and Luitz J 2001 *WIEN2K, An Augmented Plane Wave + Local Orbitals Program For Calculating Crystal Properties* ed K Schwarz Techn. Universitat, Wien, Austria ISBN 3-9501031-1-2
- [22] Hohenberg P and Kohn W 1964 *Phys. Rev. B* **36** 864
- [23] Engel E and Vosko S H 1993 *Phys. Rev. B* **47** 13164
- [24] Dufek P, Blaha P and Schwarz K 1994 *Phys. Rev. B* **50** 7279
- [25] Shannon R D 1976 *Acta Crystallogr. A* **32** 751
- [26] Barbier J 1992 *J. Solid State Chem.* **101** 249
- [27] Radosavljevic I, Howard J A K, Sleight A W and Evans J S O 2000 *J. Mater. Chem.* **10** 2091
- [28] Huang J-F and Sleight A W 1993 *J. Solid State Chem.* **104** 52
- [29] Smith R W, Kennard M A and Dudik M J 1997 *Mater. Res. Bull.* **32** 649
- [30] Chen X, Li M, Chang X, Zang H and Xiao W 2007 *J. Solid State Chem.* **180** 1658
- [31] Brown I D and Altermatt D 1985 *Acta Crystallogr. B* **41** 244
- [32] Filatov S, Shepelev Y, Bubnova R, Sennova N, Egorysheva A V and Kargin Y F 2004 *J. Solid State Chem.* **177** 515
- [33] Reshak A H, Auluck S, Majchrowski A and Kityk I V 2008 *Solid State Sci.* **10** 1445–8